NUCET NUCLEAR ENERGY AND TECHNOLOGY

Nuclear Energy and Technology 12(1): 11–18
DOI 10.3897/nucet.12.169538

Research Article

Evaluation of the excitation function for alpha particle induced reactions on the target of ^{59}Co using PACE4 code

Terefa Urgessa[1]

1 *Department of Physics, Oda Bultum University, Chiro, Ethiopia*

Corresponding author: Terefa Urgessa (terefeurgessa2022@gmail.com)

Academic editor: Zhifeng Li ♦ **Received** 22 August 2025 ♦ **Accepted** 12 January 2026 ♦ **Published** 5 March 2026

Citation: Urgessa T (2026) Evaluation of the excitation function for alpha particle induced reactions on the target of ^{59}Co using PACE4 code. Nuclear Energy and Technology 12(1): 11–18. https://doi.org/10.3897/nucet.12.169538

Abstract

Theoretical excitation functions for the alpha particle-induced reactions ^{59}Co(α,2p4n)^{57}Co, ^{59}Co(α,2pn)^{60}Co, and ^{59}Co(α,4p5n)^{54}Mn were analyzed and compared to the experimental excitation functions. Experimental cross sections were calculated using the PACE4 and TALYS-2.0 statistical model codes across an energy range of 33.1–54.5 *MeV*. PACE4 calculations used different values of level density parameters at k = 8–10, while TALYS-2.0 calculations were performed with multiple level density models (ldmodel 1–5). The analysis also examined the sensitivity and uncertainty of theoretical cross sections to changes in level density parameter. A quantitative comparison of the experimental and theoretical excitation functions was performed using calculations of reduced chi-square (χ^2_{red}) and normalized root mean square deviations (NRMSD). The findings indicate that PACE4 calculations more accurately reflect both the size and form of the experimental excitation functions compared to TALYS-2.0 calculations for the reaction channels studied. The quantitative analysis indicates the predominance of the compound nucleus reaction mechanism, suggesting that pre-equilibrium and direct contributions have a minimal impact within the energy ranges studied. This study provides a thorough justification for the nuclear theoretical models and offers consistent nuclear reaction data for alpha particle-induced reactions on a ^{59}Co target.

Keywords

Excitation Function, PACE4, TALYS-2.0, Level density parameter, χ^2_{red}, NRMSD

Introduction

The study of nuclear reaction mechanisms is one way to understand about nuclear interaction and gain information about nuclear structure (Asnain et al. 2023). The assumption made by statistical model calculations is that the decay pattern of nuclei exiting the heavy ion fusion evaporation reaction is well described. When a projectile bombards a heavy target with energy above the Coulomb barrier energy, a large number of excited nuclei are typically populated in the heavy ion fusion reaction (Ganguly and Choudhury 2020).

A foundational concept in nuclear-structure physics for a long time has been the fusion-evaporation reaction. This reaction mechanism imparts significant angular momentum and excitation energy to the nucleus (Angelis et al. 2023). Recent research indicates that various reaction mechanisms exist in heavy-ion reactions cross a range of energies, from the Coulomb barrier to much higher levels. These reactions are classified as direct, compound nucleus, and pre-equilibrium reactions (Girma and Fessahatsion 2019). The compound nucleus is formed when a projectile collides with a target nucleus, and it then decays into pairs of reaction products afterwards (Ignatyuk 2013).

Copyright *Urgessa T*. This is an open access article distributed under the terms of the Creative Commons Attribution License (CC-BY 4.0), which permits unrestricted use, distribution, and reproduction in any medium, provided the original author and source are credited.

As the compound nucleus breaks down, protons, neutrons, and other particles are released, creating the product nucleus. The term "direct nuclear reaction" refers to a nuclear reaction in which the projectile only comes into contact with the surface of the target rather than its entire nucleus (Singh 2022).

When a projectile nucleus *P* collides with a target nucleus *T*, it creates the compound nucleus CN, which has high excitation energy and is unstable. When the compound nucleus decays, it typically releases a light particle called an ejectile (*x*) and changes into a residue (R). This process can be summarized as follows:

$$P + T \rightarrow CN^* \rightarrow x + R \quad (1)$$

Where, the asterisk indicates an excitation state of the compound nucleus. *T*(*P*,*x*)*R* is the common notation for this reaction. The compound nucleus becomes sufficiently excited after one decay, due to its high excitation energy. (Castiblanco 2024). Cobalt-59 is naturally found in various ores, with a chemical symbol of Co, atomic number of 27 and atomic weight of 59. Radioactive isotopes of Cobalt are used as tracers and references for radioactive sources, as well as high-intensity radiation sources (Ditroi 2013). Cobalt-based alloys have been used as structural materials in nuclear reactors because of their exceptional strength and hardness characteristics (Yiğit 2018).

The code Pace4 formalism

The PACE (Projected Angular momentum Coupled Evaporation) code was originally developed by Gavron and has been updated to determine the value of the cross section of excited nuclei with large angular momentum that are populated in fusion evaporation reaction. It employs the Monte-Carlo simulation technique in conjunction with the statistical model approach (Ganguly and Choudhury 2020). PACE4 is built upon the Hauser-Feshbach (HF) formalism, which is included; and preconfigured with the LISE++ framework. It includes a more efficient method for coupling angular momentum during the de-excitation of excited nuclei (Kumar 2021).

The code is remarkable in that it determines the level density parameter at runtime (Ganguly and Choudhury 2020). The quantity of nuclear excited levels surrounding the excitation energy is known as the level density $\rho(E,J)$. A precise and trustworthy description of the excited states of a nucleus has been employed in the same context, to assess the effectiveness of the nuclear reaction model, which includes cross section calculations (Yiğit 2018).

There are two default level density choices that are identical to constant temperature formalism at low energies. First, the parameter "*a*" must be determined. Secondly, "*a*" is assumed to equal *A*/*K*, where *K* is a constant factor that can be adjusted to match the experimental data and *A* is the number of nucleons. The PACE4 code has the unique capability of offering data on the angular and energy distributions of evaporated particles. The distribution of projection through each cascade is tracked to obtain this. At every stage of de-excitation, the angular distribution of the particles released is ascertained (Pandey and Singh 2021).

The probability of a nuclear reaction occurring is expressed as the cross section of the reaction. When considering angular momentum (l) and specific bombarding energy, the partial cross-section for compound nucleus formation is as follows (Tarasov and Bazin 2003).

$$\sigma_l = \frac{\pi\lambda^2}{4\pi^2}(2l+1)T_l \quad (2)$$

Where, λ is the reduced wavelength and T_l is the transmission coefficient which is given by

$$T_l = \left[1 + e^{(l-l_{max})/\delta}\right]^{-1} \quad (3)$$

Where, δ is the diffuseness parameter and l_{max} is determined by the total fusion cross-section σ_F, since,

$$\sigma_F = \sum_{l=0}^{\infty} \sigma_l \quad (4)$$

TALYS-2.0

TALYS is a computer program designed for analyzing and predicting nuclear reactions. The main goal of its development is to simulate nuclear reactions involving neutrons, photons, protons, deuterons, tritons, ^{3}He- and alpha-particles, in the energy range of eV - 200 MeV for target nuclides with a mass of 12 and heavier (Koning et al. 2025). TALYS-2.0 uses the optical model code to calculate the reaction cross-section, total cross-section, the shape elastic angular distribution, inelastic cross sections and angular distributions using either a coupled-channels (deformed nuclei) or DWBA (spherical nuclei) approach and the transmission coefficients, for compound nucleus decay and pre-equilibrium emission, The level densities are calculated using the back-shifted Fermi gas model for most of the nuclides and for some of the nuclides a combined Constant Temperature + Fermi gas model is used (Pandey et.al 2021).

Tasman-2.0

TASMAN is a computer code system for nuclear data uncertainty distributions based on the nuclear model code TALYS-2.0, and for automatic optimization of the TALYS-2.0 results with respect to experimental data (Koning A 2025). The essential idea is to assume that each nuclear model parameter has its own uncertainty. Running TALYS-2.0 many times provides all needed statistical information to produce a full co- variance matrix (Koning and Rochman 2011).

Methodology

In this study, the excitation functions of the reactions ^{59}Co(α,2p4n)^{57}Co, ^{59}Co (α, 2pn)^{60} Co and ^{59}Co(α, 4p5n) ^{54} Mn were analyzed by comparing the experimental cross sections with theoretical calculations performed using the PACE4 and TALYS-2.0 codes. The experimental cross sections used in this study were obtained from the IAEA-EXFOR nuclear reaction database (EXFOR https://www-nds.iaea.org/exfor/).

Sensitivity and Uncertainty in Cross Section Calculations

PACE4 calculations were performed in the Hauser-Feshbach compound nucleus model, employing a Monte Carlo simulation to analyze the statistical decay of the excited nucleus. The parameters of the optical model for the alpha nucleus and the transmission coefficients were taken from the default PACE4 library. To assess the impact of the level density on the calculated cross sections, the parameter *k* was varied within the range of 8 to 10, which is typically used in studies on alpha particle induced reactions (Cacuci 2003).

$$\text{Sensitivity } (\backslash\%) = \frac{|\sigma(k_2) - \sigma(k_1)|}{\bar{\sigma}} \times 100 \tag{5}$$

The theoretical absolute uncertainty was calculated by

$$\Delta\boldsymbol{\sigma} = \frac{|\boldsymbol{\sigma}(k_1) - \boldsymbol{\sigma}(k_2)|}{2} \tag{6}$$

The excitation functions calculated by PACE4 were compared with experimental excitation functions to evaluate the contribution of compound nucleus processes. TALYS-2.0 calculations were performed to verify the accurate description of the reaction mechanism and the production of ^{57}Co, ^{60}Co and ^{54}Mn residues. The calculations used the same input parameters for all runs, except for the level density model, which was systematically changed. Five built-in TALYS-2.0 level density models were considered: ldmodel 1: constant temperature model, ldmodel 2: back-shift fractional flow model, ldmodel 3: generalized supersymmetric model, ldmodel 4: HFB model (HFB) dependent on temperature and ldmodel 5 — Microscopic level densities (Koning et al. 2025). For each level density model, the production cross sections of ^{57}Co, ^{60}Co and ^{54}Mn were calculated across the entire range of alpha particle. The calculations were performed by systematically varying the level density models from ldmodel = 1 to 5, while keeping all other parameters at their default settings.

For each incident energy E_i, the theoretical mean cross section was calculated as

$$\sigma_{mean}(E) = \frac{1}{N}\sum_{i=1}^{N}\sigma_i(E) \tag{7}$$

Where, $\sigma_i(E)$ is the cross section obtained with the i^{th} level density model.

The uncertainty related to the TALYS-calculated cross sections was calculated by using the standard deviation (Koning and Rochman 2012).

$$\Delta\sigma = \sqrt{\frac{1}{N-1}\sum_{i=1}^{N}\left(\sigma_i - \bar{\sigma}\right)^2} \tag{8}$$

The sensitivity of the theoretical cross section to the level density parameter was measured using TALYS-2.0 and TASMAN-2.0, with results expressed as a normalized sensitivity coefficient in percentage form. The mean absolute sensitivity takes into account differences between models, with some models exceeding the reference while others fall below it. This approach prevents the cancellation of positive and negative deviations.

$$\text{Sensitivit } (\backslash\%) = \left(\frac{1}{4}\sum_{i=2}^{5}\frac{|\sigma_i - \sigma_{ld=1}|}{\sigma_{ld=1}}\right) \times 100 \tag{9}$$

The sensitivity parameter enables the identification of energy regions where the model uncertainty is most significant, providing a direct measure of how theoretical predictions depend on level density inputs (Koning 2025).

Quantitative Comparison of the Performance of PACE4 and TALYS-2.0

A quantitative comparison was conducted to objectively validate the PACE4 and TALYS-2.0 cross section against the experimental cross section. The reduced chi-square χ^2_{red} and the normalized root mean square deviation (NRMSD) were used for this comparison. The reduced chi-square serves a measure of goodness of fit, taking into consideration experimental uncertainty. By using both reduced chi-square and NRMSD, a clear distinction can be made regarding the performance of the models in terms of size and excitation function. The reduced chi-square χ^2_{red} is defined as follows (Bevington and Robinson 2003):

$$\chi^2_{red} = \frac{1}{N}\sum_{i=1}^{N}\left[\frac{\sigma_{exp}(E_i) - \sigma_{theory}(E_i)}{\Delta\sigma_{exp}(E_i)}\right]^2 \tag{10}$$

Where, *N* is the number of experimental data points.

The following formula is used to determine the Root Mean Square Deviation (RMSD):

$$RMSD = \sqrt{\frac{1}{N}\sum_{i=1}^{N}\left(\sigma_{exp}(E_i) - \sigma_{theory}(E_i)\right)^2} \tag{11}$$

The RMSD is normalized to the experimental data range in order to obtain the NRMSD (Pomp et al. 2014).

$$NRMSD = \frac{RMSD}{\sigma_{exp,\,max} - \sigma_{exp,\,min}} \tag{12}$$

Results and discussions

The ^{59}Co(α,2p4n)^{57}Co reaction

In this reaction, an alpha particle with energy between 33.1 and 54.4 MeV would collide with the nucleus of a cobalt target, ^{59}Co. This interaction would then result in the emission of two protons and four neutrons from each reaction, ultimately forming a residue composed of ^{57Co} (Noori 2025).

The excitation function for the reaction ^{59}Co(α,2p4n)-^{57}Co was measured and compared with the calculations from TALYS-2.0 and PACE4 over the energy range of 33.1–54.5 MeV. Near the effective reaction threshold, the experimental cross section rises sharply from a low value of 7.12 mb at 33.1 MeV. Up to approximately 42–47 MeV, there is a sharp rise, and at 46.7 MeV, the cross section peaks at ~205 mb. The cross section progressively drops after this energy, reaching 138.7 mb at 54.5 MeV. The general bell-shaped trend of the excitation function is fairly well reproduced by PACE4 calculations. While PACE4 slightly underestimates the maximum value of the cross section at k = 9, PACE4 at k = 10 offers a more accurate description in the vicinity of the peak region (42.5–50.7 MeV). Although they follow the general energy dependence, TALYS-2.0 values consistently underestimate the experimental cross section in the peak region.

As shown in Fig. 1 and Table 1, at intermediate energy regions around 45–47 MeV, the reaction is governed by compound nucleus formation and the sharp increase in the excitation function. The improved agreement between the experiment and PACE4 for k = 10 shows the importance of the level density parameterization for characterizing multi-particle emission channels.

All models show significant deviations from the experimental cross section at energies above 42.5 MeV. This highlights the cross section's sensitivity to reaction thresholds, transmission coefficients, and the onset of pre-equilibrium reactions, all of which are challenging to accurately model. The experimental cross section decreases more gradually than the TALYS-2.0 calculations at higher energies (>50 MeV), indicating that pre-equilibrium emission and competing reaction channels are increasingly influential in diverting flux away from the (2p4n) exit channel.

The sensitivity and uncertainty values also indicate that model predictions are sensitive in the high-energy and peak regions. Generally, the results show that compound nucleus models provide a reasonable first-order description of the reaction.

The ^{59}Co(α,2pn)^{60}Co reaction

In this reaction, an alpha particle with an energy range between 33.1 MeV and 54.5 MeV was incident on a target composed of ^{59}Co, leading to the release of two protons and two neutrons and the formation of the residual nucleus known as ^{60}Co. (Oncology Medical Physics LLC 2019).

The PACE4 excitation functions using the level density parameters k = 8 and k = 10; are compared with the TALYS-2.0 excitation functions and the measured experimental excitation functions. Fig. 2 shows that the experimental cross section experiences a significant increase starting at 2.82 mb; reaching a peak value of 79.4 mb (≈51 MeV), before sharply rising. Following this peak, there is a slight decrease, ending at 54.5 MeV (72.46 mb). While both PACE4 and TALYS-2.0 results exhibit the general bell curve of the excitation function, notable differences are observed throughout the energy range.

From Fig. 2 and Table 2, it is evident that both PACE4 calculations significantly underestimate the experimental cross section, while TALYS-2.0 slightly overestimates it at low energies. This discrepancy indicates the strong sensitivity of the reaction yield to the onset of compound nucleus formation. TALYS-2.0 demonstrates a strong agreement with the experimental excitation function compared to PACE4 in the intermediate energy range (38–46.7 MeV). This suggests that the pre-equilibrium emission in TALYS-2.0 contributes significantly to the population of the (α,2pn) channel. The sensitivity values in this range confirm that the theoretical cross sections are highly dependent on the level density parameters. The figure also illustrates

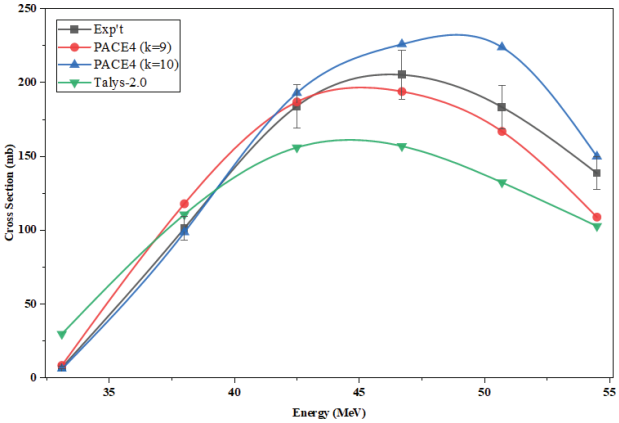

Figure 1. Excitation function of the reaction ^{59}Co(α,2p4n)^{57}Co. The vertical error bars indicate the uncertainty in the experimental cross section.

Table 1. Experimental and theoretical cross-sections for the reaction ^{59}Co(α,2p4n)^{57}Co**,** including sensitivity and uncertainty analysis

Energy (MeV)	Cross section (mb)				Sensitivity (%)		Uncertainty (±)	
	σ (Exp't)	PACE4 (k = 9)	PACE4 (k = 10)	TALYS	PACE4	TALYS	PACE4	TALYS
33.1 ± 2.65	7.12 ± 0.6	8.51	6.08	29.82	33.31	41.98	1.21	9.04
38 ± 2.45	101.39 ± 8.2	118	98.7	110.67	17.8	20.01	9.65	15.41
42.5 ± 2.25	184.03 ± 14.7	187	193	156.12	3.16	13.35	3.00	21.77
46.7 ± 2.1	205.32 ± 16.5	194	226	156.99	15.24	23.11	16	32.66
50.7 ± 2	183.44 ± 14.7	167	224	132.46	29.16	37.46	28.5	36.43
54.5 ± 1.9	138.7 ± 11.2	109	150	102.87	31.66	48.77	20	32.35

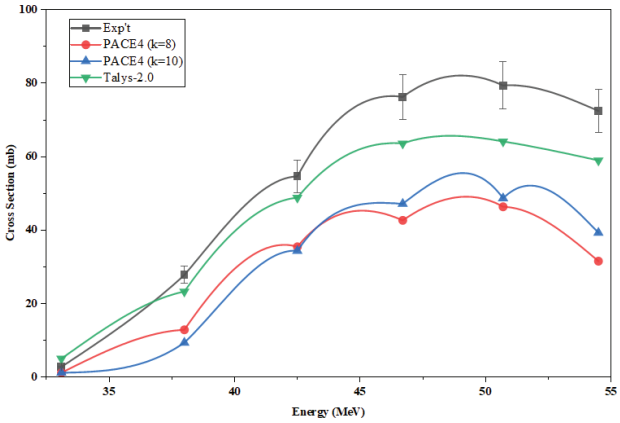

Figure 2. Excitation function of the ^{59}Co(α,2pn)^{60}Co reaction. The vertical error bars indicate the uncertainties of the experimental cross sections.

that the experimental cross section surpasses both PACE4 calculations around the peak region (46.7–50.7 MeV), while TALYS-2.0 underestimates the maximum value by 15–20%. This indicates that although compound nucleus emission predominates, the balance between neutron and proton emission is not fully reproduced by either PACE4 or TALYS-2.0.

At energies above 50 MeV, all theoretical excitation functions exhibit a decreasing trend that aligns with the experimental excitation functions. The rising uncertainties and sensitivities at these energies indicate heightened competition from other reaction channels and enhanced pre-equilibrium particle emission.

The ^{59}Co(α,4p5n)^{54}Mn reaction

In this reaction, ^{54}Mn is produced from the excited compound nucleus formed by the absorption of an incoming alpha particle by ^{59}Co; this is followed by the evaporation of four protons and five neutrons, resulting in the residual nucleus of ^{54}Mn (Ammel et al. 2010).

Fig. 3 and Table 3 show a noticeable increase in the experimental cross section from 1.76 mb at 38 MeV to a peak value of 34.48 mb at 50.7 MeV, followed by a slight decrease at higher energies. This behavior indicates the significant role of compound nucleus formation at intermediate energies. PACE4 calculations for $k = 9$ and $k = 10$ are in good agreement with the experimental cross sections with differences mostly falling within the experimental uncertainties. On the other hand, TALYS-2.0 calculations underestimate the cross sections particularly above 42 MeV. This indicates the limitations of TALYS-2.0 calculations in predicting the excitation functions the reaction compared to PACE4 calculations at lower energies.

Fig. 3 and Table 3 show that PACE4 calculations align with the excitation function for the reaction ^{59}Co(α,4p5n)^{54}Mn, confirming the effectiveness of the compound-nucleus model for this reaction channel. The strong agreement between the PACE4 results for $k = 9$ and $k = 10$ indicates that the theoretical cross sections are minimally affected by the level density parameter at energies above 46 MeV. This study is further supported by a sensitivity analysis of TALYS-2.0

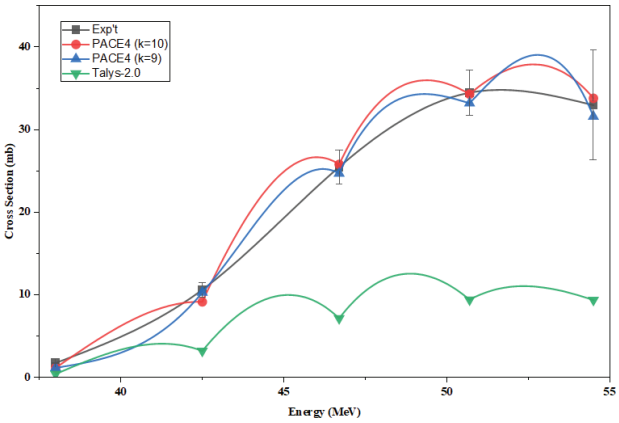

Figure 3. Excitation function of the ^{59}Co(α,4p5n)^{54}Mn reaction. The vertical error bars indicate the uncertainties of the experimental cross sections.

Table 2. Experimental and theoretical cross-sections for the reaction ^{59}Co(α,2pn)^{60}Co, including sensitivity and uncertainty analysis

Energy (MeV)	Cross section (mb)				Sensitivity (%)		Uncertainty (±)	
	σ (Exp't)	PACE4 (k = 8)	PACE4 (k = 10)	TALYS	PACE4	TALYS	PACE4	TALYS
33.1 ± 2.65	2.82 ± 0.24	1.22	1.22	5.04	0	36.94	0	1.32
38 ± 2.45	27.84 ± 2.32	12.9	9.4	23.31	31.39	35.34	1.75	7.02
42.5 ± 2.25	54.67 ± 4.4	35.5	34.4	48.85	3.15	29.29	0.5	13.69
46.7 ± 2.1	76.27 ± 6.16	42.7	47.2	63.61	10	24.19	2.25	15.45
50.7 ± 2	79.4 ± 6.4	46.4	48.7	64.15	4.8	21.54	1.15	16.51
54.5 ± 1.9	72.46 ± 5.84	31.6	39.3	59.00	21.7	19.87	3.85	16.56

Table 3. Experimental and Theoretical Cross Sections for the ^{59}Co(α,4p5n)^{54}Mn Reaction, including Sensitivity and Uncertainty Analysis

Energy (MeV)	Cross section (mb)				Sensitivity (%)		Uncertainty (±)	
	σ (Exp't)	PACE4 (k = 10)	PACE4 (k = 9)	TALYS	PACE4	TALYS	PACE4	TALYS
38 ± 2.45	1.76 ± 0.02	1.18	1.18	0.43	0	36.25	0	0.16
42.5 ± 2.25	10.63 ± 0.86	9.17	10.3	3.22	11.7	39.26	0.6	1.14
46.7 ± 2.1	25.49 ± 2.04	25.8	24.7	7.17	4.4	33.21	0.5	2.00
50.7 ± 2	34.48 ± 2.76	34.3	33.2	9.42	3.3	20.54	0.5	1.66
54.5 ± 1.9	32.97 ± 6.64	33.8	31.6	9.39	6.7	8.38	1.1	0.83

calculations, which demonstrates a decrease in sensitivity from 36.25% at 38 MeV to 8.38% at 54.5 MeV. This suggests that the model remains reliable at higher energies.

The results also indicate that TALYS-2.0 shows significantly higher sensitivity of 39.26% at an energy of 42.5 MeV; however, it reliably underestimates the experimental cross sections at higher energies. This discrepancy suggests the limitations of the TALYS-2.0 default level density parameter and pre-equilibrium processes. Conversely, PACE4 results exhibit good agreement with the experimental cross section by providing a more accurate representation of the excitation function. Therefore, the findings suggest that PACE4 offers greater predictive capability for cross-section calculations in multi-nucleon emission reactions. This indicates the necessity for enhanced modeling strategies within TALYS-2.0 to address such reaction mechanisms effectively.

Quantitative comparison of the performance of PACE4 and TALYS-2.0

Comparison of PACE4 and TALYS-2.0 for the ^{59}Co(α,2p4n)^{57}Co Reaction

As shown in Fig. 4 and Table 4, PACE4 accurately reproduces the experimental cross sections for the reaction ^{59}Co(α,2p4n)^{57}Co, indicating strong statistical agreement. The reduced chi-square values and low values of the normalized root mean square deviation (NRMSD), ranging from 8% to 9.8%, suggest that the discrepancies between theoretical and experimental cross section largely fall within the limits of the experimental uncertainty. It can be observed that for k = 9, PACE4 reproduces a slightly enhanced representation of the shape of the excitation function. In contrast, TALYS-2.0 exhibits a significantly higher reduced chi-square value of 244.5 and a higher NRMSD of 17.95%, indicating noticeable deviations from the experimental cross section. The findings confirm that PACE4 calculations provide a more suitable framework for modeling the nuclear reaction compared to TALYS-2.0.

Table 4. Reduced chi-square (χ^2_{red}) and normalized root mean square deviation (NRMSD) values for the ^{59}Co(α,2p4n)^{57}Co reaction.

Model	Reduced χ^2_{red}	NRMSD (%)
PACE4 (k = 10)	2.3	9.8
PACE4 (k = 9)	3	8
TALYS-2.0	244.5	17.95

Comparison of PACE4 and TALYS-2.0 for the ^{59}Co(α,2pn)^{60}Co reaction

Fig. 5 and Table 5 show that the PACE4 prediction for k = 10 provides the best agreement with the experimental excitation function for the reaction ^{59}Co(α,2pn)^{60}Co, with the lowest χ^2_{red} (17.7) and NRMSD (13.4%). TALYS-2.0 excitation functions exhibit the poorest agreement, with both χ^2_{red} and NRMSD, showing considerable discrepancies from the experimental excitation functions. These results confirm that the compound nucleus description used in PACE4 with k = 10 is more appropriate than both lower k values and TALYS-2.0 calculations for the reaction ^{59}Co(α,2pn)^{60}Co.

Table 5. Reduced chi-square (χ^2_{red}) and normalized root mean square deviation (NRMSD) values for the ^{59}Co(α,2pn)^{60}Co reaction.

Model	Reduced χ^2_{red}	NRMSD (%)
PACE4 (k = 10)	17.7	13.4
PACE4 (k = 8)	34	32
TALYS-2.0	35	35

Comparison of PACE4 and TALYS-2.0 for the ^{59}Co(α,4p5n)^{54}Mn Reaction

As shown in Fig. 6 and Table 6, the PACE4 calculations for k = 10 and k = 9 show excellent agreement with the experimental excitation function, with very low NRMSD values of 2.5% (k = 10) and 2.9% (k = 9). However, the large reduced chi-square value of 168 indicates significant deviations at certain energy ranges, despite small experimental uncertainties. In contrast, TALYS-2.0 calculations show a significantly higher reduced chi square (1468.5) and a high NRMSD value of 59.6%, revealing noticeable discrepancies in both magnitude and trend.

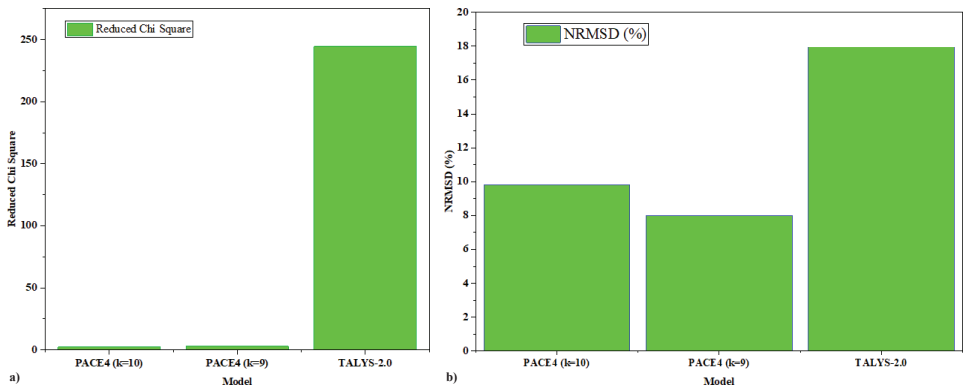

Figure 4. Statistical evaluation of model performance for the ^{59}Co(α,2p4n)^{57}Co reaction: **(a)** Reduced chi-square (χ^2_{red}) and **(b)** normalized root mean square deviation (NRMSD) for PACE4 (k = 9 and k = 10) and TALYS-2.0 calculations.

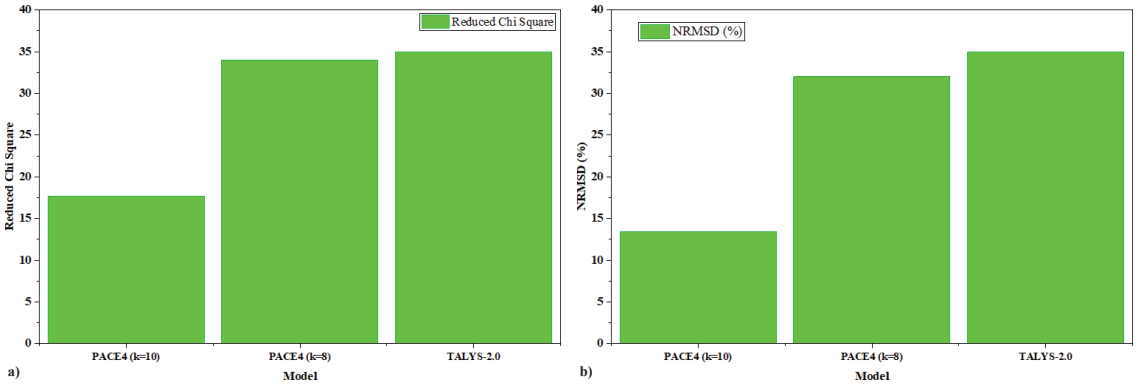

Figure 5. Statistical comparison of the performance of PACE4 and TALYS-2.0 for the ^{59}Co(α,2pn)^{60}Co reaction: Panel (**a**) displays the reduced chi-square (χ^2_{red}) values and Panel (**b**) shows the normalized root mean square deviation (NRMSD) for PACE4 (for $k = 8$ and $k = 10$) and TALYS-2.0 calculations.

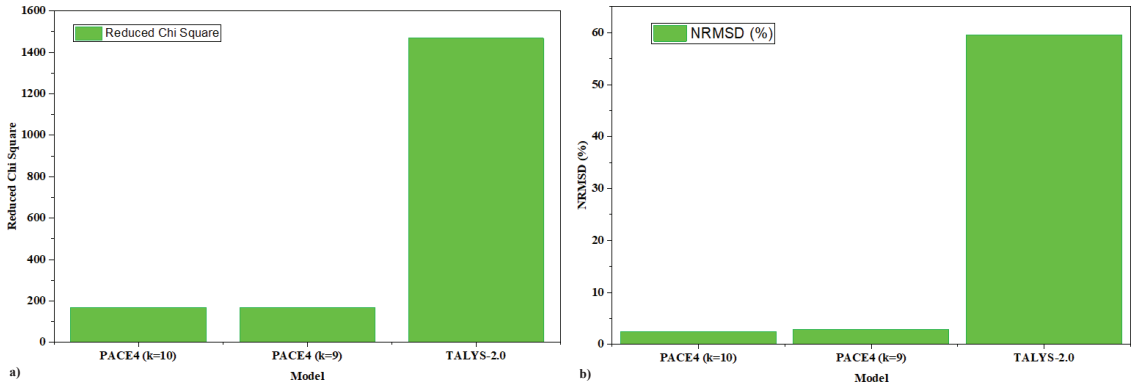

Figure 6. Statistical comparison of the performance of PACE4 and TALYS-2.0 for the ^{59}Co(α,4p5n)^{54}Mn reaction: Panel (**a**) displays the reduced chi-square (χ^2_{red}) values and Panel (**b**) shows the normalized root mean square deviation (NRMSD) for PACE4 (for $k = 10$ and $k = 9$) and TALYS-2.0 calculations.

Table 6. Reduced chi-square (χ^2_{red}) and normalized root mean square deviation (NRMSD) values for PACE4 ($k = 9$ and $k = 10$) and TALYS-2.0 calculations for the ^{59}Co(α,4p5n)^{54}Mn reaction.

Model	Reduced χ^2_{red}	NRMSD (%)
PACE4 (k = 10)	168.8	2.5
PACE4 (k = 9)	168.3	2.9
TALYS-2.0	1468.5	59.6

Overall, the results confirm that PACE4 provides a much better description of the excitation functions for the reaction ^{59}Co(α,4p5n)^{54}Mn compared to TALYS-2.0.

Conclusion

The excitation functions of the reactions ^{59}Co(α,2p4n)-^{57}Co, ^{59}Co(α,2pn)^{60}Co, and ^{59}Co(α,4p5n)^{54}Mn have been analyzed using the PACE4 and TALYS-2.0 codes. The calculations were performed within a unified model, and the influence of the level density parameters on the cross sections was investigated through sensitivity and uncertainty approaches. The results indicate a low dependence of the reaction cross section on the level density parameters as α-particle energies increase.

The quantitative comparison between PACE4 and TALYS-2.0 using the reduced chi-square and NRMSD values reveals that PACE4 provides significantly superior results compared to TALYS-2.0 for all reaction channels. This finding suggests that the compound nucleus reaction mechanism, well captured by PACE4, dominates in high-multiplicity particle emission reactions. In contrast, TALYS-2.0 tends to underestimate the experimental excitation functions, indicating limitations in its handling of level density and pre-equilibrium effects for the reaction channels.

The finding confirms the reliability of PACE4 for modeling alpha particle-induced reactions on cobalt-59 and establishes solid foundation for its use in calculating reaction cross-section when experimental data is not available.

Data availability

The data underpinning the analysis reported in this paper are deposited in Zenodo at https://doi.org/10.5281/zenodo.18283073.

Acknowledgments

The author would like to express gratitude to Oda Bultum University for their assistance in providing the necessary materials to complete this work.

References

- Ammel V, Paepen J, Pommé S, Sibbens G (2010) Measurement of the ^{54}Mn half-life. Applied Radiation and Isotopes 68(12): 2387–2392. https://doi.org/10.1016/j.apradiso.2010.06.010
- Angelis D, Benzoni G, Cederwall B, Korichi A, Leoni S, López-Martens A, Nyberg J, Paul S, Valiente-Dobòn J (2023) Nuclear structure advancements with fusion-evaporation reactions. The European Physical Journal A 59(7): 144. https://doi.org/10.1140/epja/s10050-023-01032-5
- Asnain S, Sharma K, Shuaib M, Siddique A, Bhat M, Singh B, Prasad R (2023) Investigating the influence of input angular momentum on independence hypothesis in heavy-ion induced fusion reactions. Nuclear Physics A 1041: 122786. https://doi.org/10.1016/j.nuclphysa.2023.122786
- Bevington PR, Robinson DK (2003) Data Reduction and Error Analysis for the Physical Sciences (3rd edn.). McGraw-Hill. https://doi.org/10.1119/1.17439
- Cacuci DG (2003) Sensitivity & Uncertainty analysis: Theory. Chapman and Hall/CRC. https://doi.org/10.1201/9780203498798
- Castiblanco D (2024) Cross section estimation for heavy ion nuclear reactions with a cascade code of fusion evaporation. Momento 68: 52–68. https://doi.org/10.15446/mo.n68.106810
- Ditroi F, Tarkanyi F, Takacs S, Hermanne A, Yamazaki H, Baba M, Mohammed A (2013) Activation cross section of longer-lived products of proton induced nuclear reactions on Cobalt up to70MeV. Journal of Radio-analytical and Nuclear Chemistry 298(2): 853–865. https://doi.org/10.1007/s10967-013-2578-8
- Ganguly S, Choudhury T (2020) The Dominance of Proton/Neutron Evaporation Exit-Channel in a Fusion-Evaporation Reaction: The Effect of Target Nuclear Ratio (N/Z). International Journal of Innovative Technology and Exploring Engineering 9(6): 456–457. https://doi.org/10.35940/ijitee.f3732.049620
- Girma A, Fessahatsion G (2019) Investigating entrance channel influences in the fusion of some heavy–ion systems. Journal of Applied Biotechnology & Bioengineering 6(5): 247–525. https://doi.org/10.15406/jabb.2019.06.00200
- Ignatyuk A (2013) Statistical theory of nuclear reactions. ICTP-IAEA Joint Workshop on Nuclear Data for Science and Technology: Medical Applications. Institute of Physics and Power Engineering. Obninsk, Russia.
- Koning A (2025) TASMAN-2.2 Statistical software for TALYS: Uncertainties, sensitivities and optimization. https://nds.iaea.org/talys/tutorials/tasman.pdf
- Koning AJ, Rochman D (2011) Modern Nuclear Data Evaluation: Straight from Nuclear Physics to Applications. Journal of the Korean Physical Society 59(2(3)): 773–778. https://doi.org/10.3938/jkps.59.773
- Koning A, Hilaire S, Goriely S, IAEA (2025) TALYS-2.2. https://nds.iaea.org/talys/tutorials/talys.pdf
- Koning A, Rochman D (2012) Modern Nuclear Data Evaluation with the TALYS Code System. Nuclear Data Sheets 113(12): 2841–2934. https://doi.org/10.1016/j.nds.2012.11.002
- Kumar R, Maiti M, Sarkar G, Sagwal M, Kaur P, Prajapat R, Nag T, Sodaye S (2021) Study of excitation functions and insights into the reaction mechanisms of ^{6}Li fusion in Cu. The European Physical Journal A. Hadrons and Nuclei 57(6): 209. https://doi.org/10.1140/epja/s10050-021-00520-w
- Noori S (2025) Modeling Excitation Functions for Cobalt-57 Production Using natural Iron-Nickel-Copper Targets for Medical Applications. Muthanna Journal of Pure Science 12(1): 49–62. https://doi.org/10.52113/2/12.01.2025/49-62
- Oncology Medical Physics LLC (2019) Cobalt-60. https://oncology-medicalphysics.com/cobalt-60/
- Pandey K, Singh D (2021) Evaluated $^{149,152,155\ \&161}$Tb production cross-sections using Gd(p, xn)Tb reactions near and above threshold. Thesis. Journal of Nuclear Medicine & Radiation Therapy 12: 456. https://www.hilarispublisher.com/open-access/evaluated-149152155-161tb-production-crosssections-using-gdp-xntb-reactions-near-and-above-thershold.pdf
- Pandey K, Singh DP (2021) Evaluated $^{149,152,155\ \&161}$Tb production cross-sections using Gd(p, xn)Tb reactions near and above threshold. Journal of Nuclear Medicine & Radiation Therapy 12: 10. https://www.hilarispublisher.com/open-access/evaluated-149152155-161tb-production-crosssections-using-gdp-xntb-reactions-near-and-above-thershold.pdf
- Pomp S, Koning AJ, Rochman D (2014) On the use of statistical methods for the evaluation of nuclear data. Nuclear Data Sheets 119: 218–221.
- Singh A (2022) Study of nuclear reaction and nuclear decay modes using relativistic mean-field theory. PhD Thesis. Rajiv Gandhi Institute of Petroleum Technology Jais, India – 229304. https://doi.org/10.1016/j.nuclphysa.2022.122439
- Tarasov O, Bazin D (2003) Development of the program LISE: Application to fusion evaporation. Nuclear Instruments and Methods in Physics Research Section B: Beam interaction with Materials and Atoms 204: 174–178. https://doi.org/10.1016/S0168-583X(02)01917-1
- Yiğit M (2018) Theoretical study of cross sections of proton-induced reactions on cobalt. Nuclear Engineering and Technology 50(3): 411–415. https://doi.org/10.1016/j.net.2018.01.008